H2Open Journal

H_2Open Journal Vol 6 No 1, 1 doi: 10.2166/h2oj.2023.044

Water infiltration rate in the Kathmandu Valley of Nepal amidst present urbanization and land-use change

Ganga Shrestha [a,b], Bijay Man Shakya [c], Mohan Bikram Shrestha[b] and Udhab Raj Khadka[a,*]

[a] Central Department of Environmental Science, Tribhuvan University, Kathmandu, Nepal
[b] Wildlife Research and Education Network (WREN), Kathmandu, Nepal
[c] Smartphones for Water Nepal (S4W-Nepal), Lalitpur, Nepal
*Corresponding author. E-mail: ukhadka@cdes.edu.np

GS, 0000-0003-0349-9145; BMS, 0000-0001-5421-5742

ABSTRACT

The rapid urbanization and land-use change prominently decreased groundwater recharge areas. Infiltration occurring through permeable areas is responsible for groundwater recharge. However, detailed studies of infiltration in low-income countries especially in human-encroached recharge areas are limited. Thus, this study mainly aims to measure the infiltration rate in the major recharge areas of the Kathmandu Valley (KV) using a double-ring infiltrometer (concentric ring size 30 and 15 cm). It also aims to estimate the volume of groundwater recharge with respect to the decrease in permeable areas in the northern part of the KV. The results revealed the infiltration rate ranging from 0.01 to 37.2 cm/h with an average of 7.3 $\pm$ 8.4 cm/h. The infiltration is found to be dependent upon land-use among different categories and organic matter among different soil properties. Additionally, the volume of water recharge in 2010, 2020, and 2030 was estimated as 67.73, 59.05, and 51.5 million cubic meters per year (MCM/year), respectively, which clearly showed a decrease in water recharge with respect to a decrease in the permeable areas. Hence, the findings would be useful for policymakers, stakeholders, and urban planners regarding the preservation and conservation of permeable areas for sustainable water resource management and urban flood management.

Key words: double-ring infiltrometer, groundwater recharge, infiltration test, steady condition

HIGHLIGHTS

- The importance of permeable land for groundwater recharge and sustainable water resource management.
- Up to now, there are no data for the infiltration rate of the Kathmandu Valley.

INTRODUCTION

Groundwater is the primary source of water for 2 billion people around the world (Alley *et al.* 2002). Despite its importance, most aquifers are experiencing rapid rates of groundwater depletion (Konikow & Kendy 2005). Due to combined anthropogenic and environmental processes, there is a high complexity of groundwater management which once degraded is difficult to repair (Jakeman *et al.* 2016). There are many factors that amplify its degradation, namely population growth, land-use and land-cover (LULC) change, climate change, and others (Gosling & Arnell 2016; Weber & Sciubba 2018; Olivares *et al.* 2019). However, change in land-cover is expected to lower recharge and deplete groundwater levels even more (Scanlon *et al.* 2005; Mishra & Kumar 2015). Hence, in order to ensure the sustainability of groundwater, a better understanding of the impact of land-use and the amount of water recharge is needed.

There are different approaches to assessing the impact of LULC change on groundwater recharge. For example, experimental methods such as isotopic tracers (Wang *et al.* 2008), statistical approaches like water-table fluctuation analysis (Moon *et al.* 2004), and numerical methods like water balance simulation (Batelaan *et al.* 2003) are in use. However, the methods are costly and time constraining. Effective infiltration is yet another type of method used mainly for the permeability of surface deposits (Paczynski 1995; Stasko *et al.* 2012).

Infiltration is one of the important contributing factors to groundwater recharge. Estimation of infiltration in the field has always proved to be difficult. Therefore, most of the available estimates are based on theoretical calculations, considering parameters like slope, characteristics of soils, amount and duration of rainfall, runoff, etc.

Whereas, some approaches have been adopted to quantify rate in the field using portable rainfall simulators (Harden & Scruggs 2003): double-ring infiltrometer (Osuji *et al.* 2010; Wang *et al.* 2018; Shrestha & Kafle 2020), mini-disc infiltrometer (Kumar *et al.* 2021), single-ring infiltrometer (Verbist *et al.* 2010), artificial precipitation simulator (Wang & Zhang 1991), run off-on ponding techniques (Bobe 2004), etc. Nevertheless, the infiltration method is advantageous as it incorporates other processes such as the movement of water within the soil (Turner 2006), soil physical properties (Walker *et al.* 2006; Rashidi & Seyfi 2007), surface soil compaction (Yimer *et al.* 2008), vegetation coverage, and types (Molina *et al.* 2007). Although, the infiltration method is sensitive, it is easy to understand and cost-effective and easy mobility makes it useful to researchers in developing countries.

In general, population growth and urbanization are two main drivers for increasing water demand globally (Bradley *et al.* 2002; McDonald *et al.* 2011); meanwhile South-Asian countries are suffering from the reduced groundwater infiltration with increased concrete pavements. Meanwhile, countries in the South-Asian region are highly dependent on groundwater. The problem is huge in those areas where the watershed is isolated, with groundwater being a major component of water resources. The Kathmandu Valley (KV) of Nepal is no exception, having an isolated watershed combined with a population boom and change in land-use patterns.

The sole domestic water supplier in the KV, the Kathmandu Upatyaka Khanipani Limited (KUKL), fulfils 60–70% of the water demand in the dry season and nearly half in the wet season using groundwater sources, causing water scarcity and increased dependency on shallow and deep groundwater (Shrestha & Shah 2014). Consequently, this valley has witnessed water-table decline due to over extraction (Shrestha 2009; KVWSMB 2012; Gautam & Prajapati 2014). Due to unprecedented LULC change in the valley, the recharging areas are also being affected, as it transforms permeable land (open vegetated areas) to impervious (concrete buildings and infrastructure) (Zhou *et al.* 2013) resulting in increased surface runoff and loss of groundwater recharge areas (Lamichhane & Shakya 2019). The decrease in infiltration amidst over-extraction of groundwater is making the valley vulnerable to land subsidence (Pandey *et al.* 2010; Gautam & Prajapati 2014).

Based on the groundwater recharge potential, the KV is divided into three different groundwater districts, i.e., Northern, Central, and Southern districts. Among the districts, the Northern District has comparatively high groundwater recharge potential (Shrestha & Shah 2014; Dahal *et al.* 2019; Shakya *et al.* 2019). Different groundwater modeling has been adopted to study hydrology and groundwater dynamics of the KV (Sonaje 2013; Dahal *et al.* 2019; Lamichhane & Shakya 2019, 2020). However, there seems to be very scarce previous works on groundwater recharge based on the field experiments. Since the land-use pattern of the KV is changing rapidly, the infiltration capacities of the critical locations considered as the groundwater recharge are to be considered for the future land-use pattern and water management practice. The present work aims to determine the infiltration rate using simple cost-effective infiltration methods in changing land-use in the northern recharge areas (JICA 1990) of the KV. Depending upon land-use, soil types, soil texture, and geological formation, this study is aimed at understanding the relationship between infiltration rate and soil parameters along with estimating the groundwater recharge volume by predicting the land-use change pattern for 2010, 2020, and 2030 in the KV for effective water management.

MATERIALS AND METHODS

Study area

The Northern Groundwater District lies in the KV, Nepal within 27°32′13″ N to 27°49′10″ N latitude and 85°11′31″ E to 85°31′38″ E longitude. Within the Northern Groundwater District, Tokha Municipality, Budhanilkantha Municipality, Gokarna Municipality, Kageshwori-Manohara Municipality, Shankharapur Municipality, and Tarkeshwor Municipality were selected as the representative sites, covering an area of 77.4 km^2 (Figure 1). Geologically, these areas are under Tokha and Gokarna formations, which have medium to moderately higher potential for groundwater recharge (JICA 1990; Pandey & Kazama 2011). The zone is dominated mainly by coarse sediments deposited by lakes and rivers (Shakya *et al.* 2019). Hydrogeologically, the area is considered as the groundwater recharge zone of the KV (JICA 1990).

The study area encompasses cultivated land, built-up areas, and non-cultivated land. The cultivated land covers seasonal crops, irrigated, or non-irrigated farms with main seasonal crops including paddy, wheat, barley, potato, chili, onion, garlic, maize, etc. The built-up or settlement areas cover all types of impervious (or very little

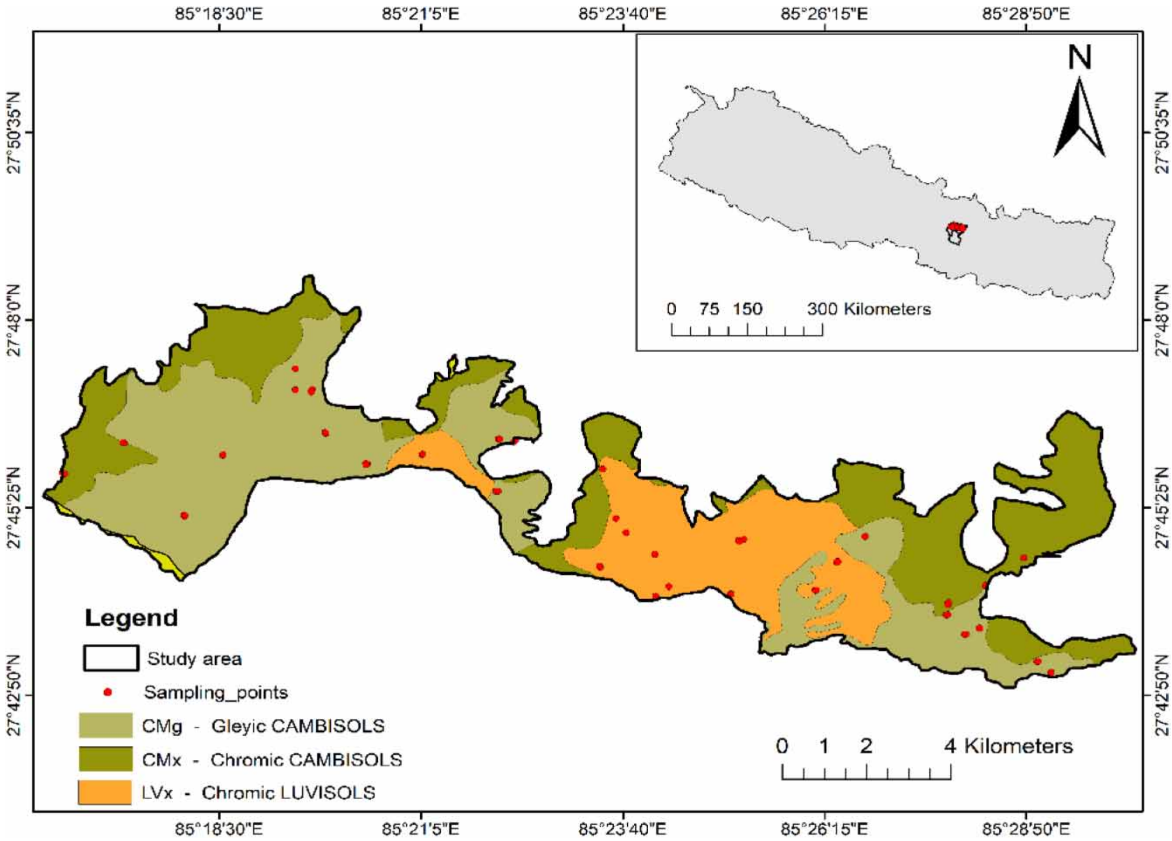

Figure 1 | Location of the study area (upper right) and sampling sites (lower).

pervious) land consisting of paved streets, residential buildings, highways, and commercial areas. The non-cultivated land includes areas with natural vegetation and regeneration, and open areas.

METHODS

Determination of the infiltration rate

A proportional sampling method was used in this study to determine the number of sampling points. Altogether, 85 sites were selected based on the soil types, i.e., Gleyic cambisols-44, Chromic cambisols-11, and Chromic luvisols-30) as described by Dijkshoorn & Huting (2009). A double-ring infiltrometer with two concentric rings having diameters of 15 and 30 cm for inner and outer rings, respectively, and 25 cm of height was used to measure the infiltration rate (Setiawan *et al.* 2019). The set up was driven up to 10 cm for both rings using a hammer (Farid *et al.* 2019) (Figure 2(a)). The utmost care was taken to minimize the disturbance of soil surface inside the rings at the time of installation as well as when pouring water into the rings. Water was poured in both the rings together up to 15 cm above the surface soil. The recordings were within time differences of 1, 2, 4, 5, 10, 20, 30 min and further were carried out until a steady infiltration condition was attained (Figure 2(b)). The constant infiltration rate was obtained after some hours, which is considered to be a steady infiltration rate (*Bi*) (Supplementary material, Annex 1). The total amount of water infiltrated at a given time is called cumulative infiltration (*Ci*). The steady rate was assumed to have been achieved when similar values appeared in two consecutive infiltration rates during the measurement. Measurement of the inner ring was only recorded in this study as the purpose of the outer ring was just to suppress the lateral percolation of water from the inner ring (ASTM 2003). In most of the sites, three replicate measurements were taken, whereas in some sites only two replicates were measured.

The method of determining infiltration rate using a double-ring infiltrometer has been adopted by many researchers in different regions of the world (Bean *et al.* 2004; Igboekwe & Adindu 2014; Lamichhane & Shakya 2019; Mahapatra *et al.* 2020), making it cost-effective and result orientated.

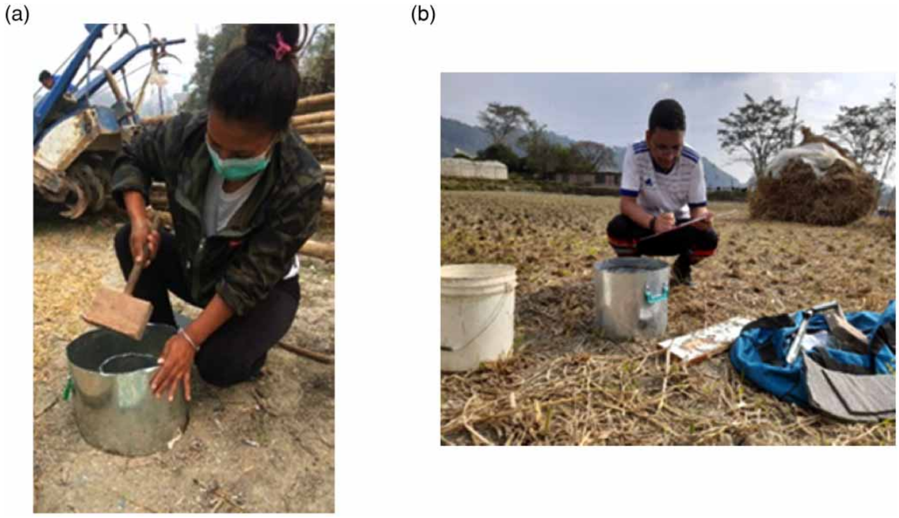

Figure 2 | (a) Inserting double-ring infiltrometer and (b) measuring infiltration rate.

Infiltration parameters like sorptivity (S) and saturated hydraulic conductivity (K_{sp}) were determined using the Philips infiltration model (Orjuela-Matta *et al.* 2012; Masoud *et al.* 2019). Philip (1957) fits two parameters, i.e., sorptivity and saturated hydraulic conductivity, to describe infiltration rate in relation to time. The Philips equation can be expressed as:

$$I(t) = St^{1/2} + K_{sp}t \quad (1)$$

where S is the sorptivity and describes absorption by the soil (cm/h$^{0.5}$); K_{sp} describes the saturated hydraulic conductivity (cm/h).

The fit of Equation (1) was carried out in simple linear regression in MS-Excel.

Soil sample preparation and analysis

The undisturbed soil samples from the sampling points were collected using a soil auger at depth of 0–20 cm. The upper horizon of soil has direct exposure to natural and anthropogenic changes along with high organic content and nutrient reserves (Tiwari *et al.* 2006). Hence, for the present study, soil-depth up to 20 cm was considered. Soil samples were separately collected for calculating bulk density and moisture content, pH, texture, and organic matter. For the physical and chemical properties, sampled soils were air dried for 2 weeks, gently crushed, and stored in clean polythene bags which were later passed through a 2-mm sieve for further lab analysis.

The various soil parameters were determined using standard methods. The bulk density was determined using the core sampler with measurement (radius and height of core being 1.8 and 4 cm, respectively) (Grossman & Reinsch 2002) and moisture content determined using the oven dry method. The soil pH was determined using a 1:5 soil–water ratio with a Milwakee pH probe. Likewise, organic carbon was determined using Walkley and Black wet oxidation methods (Nelson & Sommers 1982). Organic matter was calculated by a factor of 1.72 (Van Bemmelen's Correction Factor) (Waxman & Stevens 1930). The soil texture was determined using the Bouyoucos hydrometer method (Gee & Bauder 1986).

Estimation of groundwater recharge

Shallow aquifers are generally recharged through an infiltration process. The volume of groundwater recharge was estimated using steady infiltration rate with a hypothesis of average infiltration rate being constant over time (the obtained infiltration rate for estimation of the recharge volume was only for shallow groundwater recharge, not the deep recharge). For the calculation of volume of groundwater recharge, the total area of recharging zone (permeable areas) of the northern belt was calculated by ArcGIS 10.2.1. The aggregate recharge for a drainage basin is the sum of the recharge values for each precipitation area as shown in the following equation.

$$\text{Groundwater recharge } (R) = a_r * A_r \tag{2}$$

where a_r is the average infiltration rate for the precipitate area (effective fraction); A_r is the surface area of recharge area.

The data collected from the field were arranged, organized, and analyzed using Spearman's rank correlation, Mann–Whitney *U* test, and Kruskal Wallis test. Multivariate analysis such as principal component analysis (PCA) (Tiwari *et al.* 2006; Abdel-Fattah *et al.* 2021) and cluster analysis (Cupak *et al.* 2017) were carried out. All analyses were carried out in MS-Excel, IBM SPSS Statistics 23.0, and ArcGIS 10.2.1.

RESULTS AND DISCUSSION

Infiltration rate

The present study revealed that the steady infiltration rate varies considerably from 0.01 to 37.2 cm/h with an average of 7.3 cm/h (Figure 4). Setiawan *et al.* (2019) reported steady infiltration rate variation from 5.4 to 63.93 cm/h in the Lombok Island, Indonesia. Other researchers (Chen *et al.* 2014; Patle *et al.* 2018; Wang *et al.* 2018) also reported the similar findings. Meanwhile, various researchers reported infiltration rates different from the current study. The various infiltration rates are presented in Table 1. These kinds of variation in steady infiltration rate are presumed to be from the root and faunal microspores that exist in association with the land-use and variety of crop species (Harden & Scruggs 2003). Also, adoption of varying ring type and its diameter made it different from other studies' findings.

Table 1 | Comparison of infiltration rates along with methodologies

				Ring size (cm)			
S.No.	**Country**	**References**	**Ring type**	**Diameter**	**Height**	**ID**	**IR**
1	India	Kadam (2016)	SR	10	13	3	2.65–6.73
2	Spain	Cerda (1996)	SR	7	15	6	25.6–46.8
3	India	Mahapatra *et al.* (2020)	DR	30/60	NA	10	0.08–10.51
4	Kenya	Mireille *et al.* (2019)	DR	NA	NA	15	7.88–89.14
5	China	Wang *et al.* (2018)	DR	NA	5.2	10	0.23–25.50
6	Indonesia	Kusumandari & Marpaung (2019)	DR	NA	NA	NA	3.6–11.2
7	India	Nileshwari *et al.* (2016)	DR	30/60	NA	10	4.34–6.06
8	Spain	Neris *et al.* (2020)	DR	25/50	25	10	6.7–79.6
9	Nepal	Present Study	DR	15/30	25	10	0.01–37.2

SR, single ring; DR, double ring; IR, infiltration rate (cm/h); ID, inserted depth (cm).

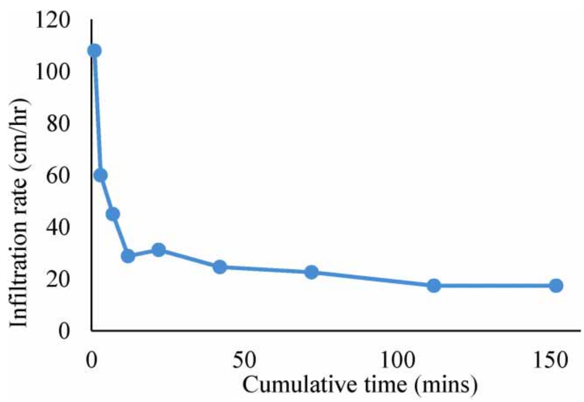

Figure 3 | Graph showing the infiltration rate to obtain steady state.

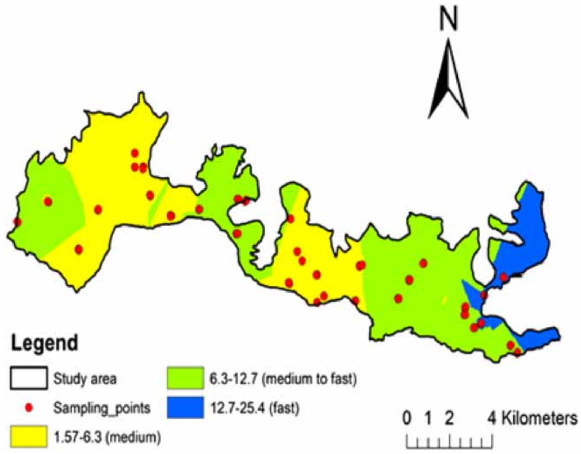

Figure 4 | Interpolation of the infiltration rate. Please refer to the online version of this paper to see this figure in colour: http://dx.doi.org/10.2166/h2oj.2023.044.

In the current study, the infiltration trend is found to be in descending order and the difference between the initial and final infiltration rates was quite large (Figure 3). The infiltration rate was highest at the very beginning of the experiment, tended to decrease steadily at different rates and stages, and reached about steady state, which is considered to be the steady infiltration rate (Yasin & Ghazal 2021). Horton (1933) explained this phenomenon in which infiltration capacity decreases with time until it approaches a constant infiltration rate. At the initial time of infiltration process, water flows rapidly before the soil gets wet, and later the flow slowly decelerates as the clay expands increasing the soil porosity while reducing the infiltration rate (Setiawan *et al.* 2019).

In terms of steady state in the present study, it was achieved maximally between the time period 102 and 121.8 min (1.7 and 2.03 h, respectively) (Figure 3). Diamond & Shanley (2010) reported the steady infiltration rate at 4.5–7.5 h in winter and from 6.5 to 8.5 h in summer. The reason for the differential time required to achieve steady state may be due to different spatial and temporal conditions.

According to Kohnke (1968) classification, in the present study, the infiltration rates fall in different categories, i.e., 3.5% in very slow, 9.4% in slow, 25.9% in slow to medium, 23.5% in medium, 11.8% in medium to fast, 20% in fast, and 5.9% in very fast. The interpolated map (Figure 4) shows high infiltration rate in the Sankhu area (blue color). Areas like Gagalphedi, Budhanilkantha, and some parts of Tarkeshor (green color) have medium to fast infiltration rates. The areas such as Gokarna, Tokha and Tarkeshwor (yellow color) have medium infiltration rates (Figure 4). Dahal *et al.* (2019) reported similar results from the northern part of the KV which includes areas like Lapsephedi, Gagalphedi, Nayapati, Sundarijal, Chapali, Bhadrakali, Budhanilkantha, and Baluwa, validating the results of the current study.

Infiltration rate is dependent upon soil types (Chromic cambisols, Chromic luvisols, and Glyeic cambisols), soil texture (sandy and sandy loam), and geological formation (Tokha and Gokarna formation). However, the current study does not show significant differences in infiltration rate. Loague & Gander (1990) have also found no variation in infiltration rate in varied soil textures. In KV, both the formations (Tokha and Gokarna) are considered to have potential for groundwater recharge (Shrestha & Shah 2014). Yet, the overall land-use (cultivated and non-cultivated land) showed significant differences ($P < 0.05$, $P = 0.004$) in the infiltration rate. Several studies (Osuji *et al.* 2010; Neris *et al.* 2020) have also shown significant variation in the infiltration rates with the different land-use types. The present results show higher infiltration rate in cultivated land than in non-cultivated land (Figure 5). This result is similar to those of Nileshwari *et al.* (2016) and Wang *et al.* (2018) where a higher infiltration rate was found in cultivated land compared to the non-cultivated land. Vegetated area in cultivated land has organic matter which promotes a crumbly structure and improves the permeability of the soil (Haghnazari *et al.* 2015). Meanwhile, the micro topographic forms at the soil surface increase the residence times of water in the soil and promote infiltration (Danin & Barbour 1982). Non-cultivated lands are disturbed and trampled by humans, resulting in loss of understory vegetation and leading to serious problems like Horton overland flow and soil erosion (Linh *et al.* 2018). Therefore, the rate of infiltration will be less in non-cultivated land than any other cultivated lands. The high range of variation of infiltration rate in cultivated land is assumed to be due to

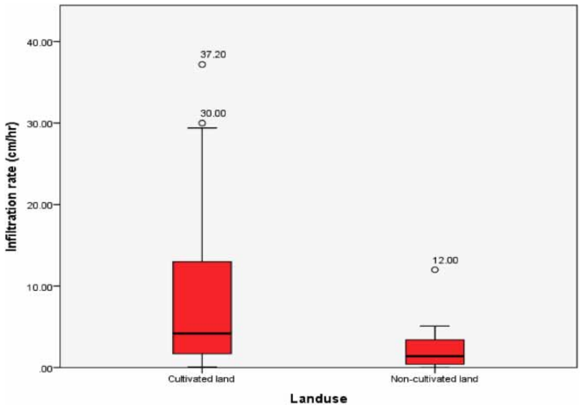

Figure 5 | Infiltration rate by land-use.

differences in vegetation composition, since it plays an important role in soil organic matter, soil microbial community and soil quality (Hou *et al.* 2012). Also, different types of cropping patterns have different rates of deep percolation. For example, rice fields have 59% and wheat have 5.6% which might result in variation in infiltration rates (Tyagi *et al.* 2000a, 2000b). Additionally, variation in agricultural practices also affects the infiltration rate. For instance, the use of heavy machines to plow the field leads to increased compaction as well as bulk density and tends to cause low infiltration rate (Chancellor 1977).

Infiltration rate and soil properties

The results showed a significant positive correlation ($r = 0.287$, 0.01) between infiltration rate and organic matter, whereas other parameters showed no significant correlation (Table 2). Several studies also found a significant positive relation between infiltration rate and organic matter (Osuji *et al.* 2010; Haghnazari *et al.* 2015; Wang *et al.* 2018). Soil organic matter was considered to be the chief component for determining soil quality (Tiwari *et al.* 2006), hence the soils with high infiltration rates are of good quality index due to high organic content. During the dry season, soil moisture decreases resulting in an increase in absorption capacity (sorptivity) of soil and cumulative infiltration (Yasin & Ghazal 2021). However, in the present study, there seems no apparent impact of soil moisture content on the basic infiltration.

The result of the Kaiser Meyer Olkin (KMO) measure of sampling adequacy and Bartlett's sphericity test during the PCA gave a value 0.613. The eigenvalue greater than 1 was considered for the number of components that

Table 2 | Correlation between parameters

	Bi	Ci	S	K_{sp}	pH	Moisture	Bulk	Sand	Silt	Clay	SOM
Bi	1.000										
Ci	0.949**	1.000									
S	0.619**	0.709**	1.000								
K_{sp}	0.018	−0.084	−0.628**	1.000							
pH	−0.154	−0.150	−0.253*	.212	1.000						
Moisture	−0.**034**	−0.**067**	−0.**276***	0.243*	0.032	1.000					
Bulk	−0.198	−0.156	−0.083	0.020	0.120	−0.018	1.000				
Sand	−0.049	−0.056	−0.121	0.143	0.278*	0.093	−0.193	1.000			
Silt	0.018	0.028	0.114	−0.184	−0.331**	−0.063	0.105	−0.971**	1.000		
Clay	0.083	0.084	0.061	0.115	0.117	−0.150	0.365**	−0.325**	0.116	1.000	
SOM	0.**287****	0.230*	0.063	0.053	−0.234*	0.008	−0.315**	0.010	0.006	−0.168	1.000

*Correlation is significant at the 0.05 level (two-tailed).
**Correlation is significant at the 0.01 level (two-tailed).

Table 3 | Rotated component matrix

Rotated component matrix

	Component		
Attributes	**1**	**2**	**3**
Bi	0.318	0.841	0.171
Ci	0.528	0.754	0.086
S	0.931	0.220	0.118
K_{sp}	−0.917	−0.068	−0.129
Moisture	−0.258	0.118	−0.173
Bulk	0.092	−0.438	0.582
Sand	−0.087	−0.115	−0.703
Clay	0.181	0.096	0.805
SOM	−0.292	0.693	−0.096
Eigenvalue	3.074	1.774	1.066
% of variance	34.158	19.708	11.843
Cumulative %	34.158	53.866	65.709

study the variation and resulted in three components from nine variables which contributes 65.71% of the total variance. According to factor loading, PC1, PC2, and PC3 explained 34.15, 19.71, and 11.84% of the total variance, respectively (Table 3).

The highly weighted parameters in PC1 were sorptivity (*S*), moisture, and saturated hydraulic conductivity (K_{sp}). In PC2, high loaded values were basic infiltration rate, cumulative infiltration, and soil organic matter. Likewise, in PC3, clay, sand, and bulk represent the highest loading value. The PC1 and PC2 directly explain the infiltration characteristics, whereas PC3 did not. They showed organic matter and infiltration rate (*Bi* and *Ci*) in the same component (PC2), which signifies that the infiltration rate is chiefly governed by soil organic matter (Figure 6). Alhassoun (2009) also stated that soil biological properties (earthworm biomass, its abundance, and dehydrogenase activity) contribute directly to the infiltration rate. Using the multivariate tool PCA, Setiawan *et al.* (2019) revealed a strong correlation of infiltration rate with soil physical properties such as soil moisture, particle size distribution, and bulk density other than soil organic matter in that study.

The hierarchical clustering of sampling points showed three clusters mainly based on land-use. Cluster-1 is dominated by land left after the paddy harvest, cluster-2 by barren land, and cluster-3 by vegetables (onion,

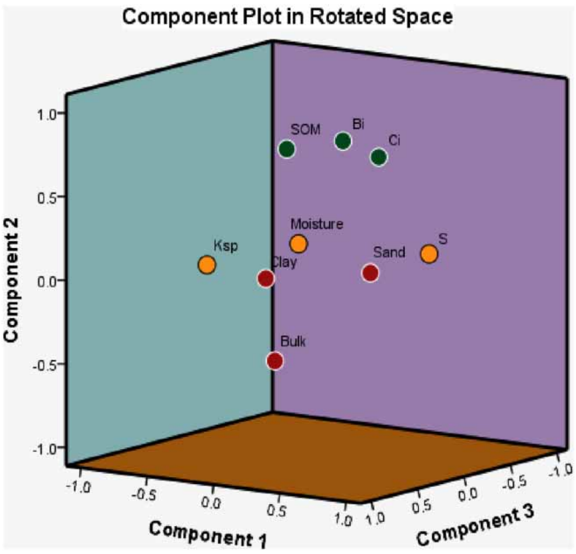

Figure 6 | Principal component analysis.

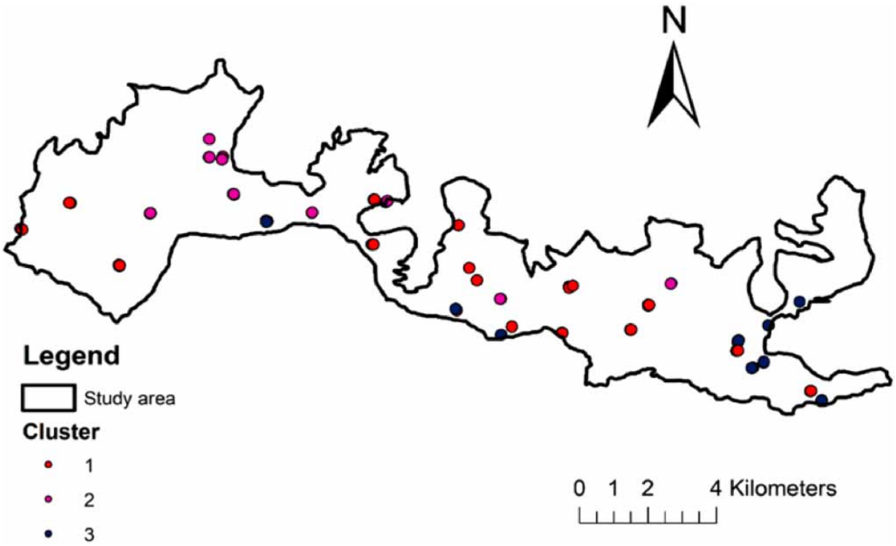

Figure 7 | Clustering of sampling points.

garlic, spinach, cabbage, etc.) grown area (Figure 7). The variation in infiltration rates among the different sites in this study area is hence governed by soil parameters, which are directly or indirectly related to the types of plants grown, or root system of the plants as well as the compaction of soil due to human trampling.

Groundwater recharge

Change in land-use from permeable to impermeable due to urbanization can be easily seen in the present study area (Figure 8). The conversion percentage of permeable to impervious land was 11.78%, which was slightly greater than Dahal *et al.* (2019) and reported 10.6% for 1996–2011 and 12.2% for 2011–2030 in the KV. Lamichhane & Shakya (2019) estimated at least 6% of the open areas being encroached upon for built-up areas in each decade.

Land conversion from permeable to non-permeable built-up areas has declined the volume of water that infiltrates into the ground by 8.68 million cubic meters per year (MCM/year) in 2020 and is projected to decline by 7.55 MCM/year in 2030. In 20 years, i.e., from 2010 to 2030, 16.23 MCM/year loss has been estimated (Table 4). The decline in groundwater recharge due to the LULC change is also supported by Lamichhane & Shakya (2020)

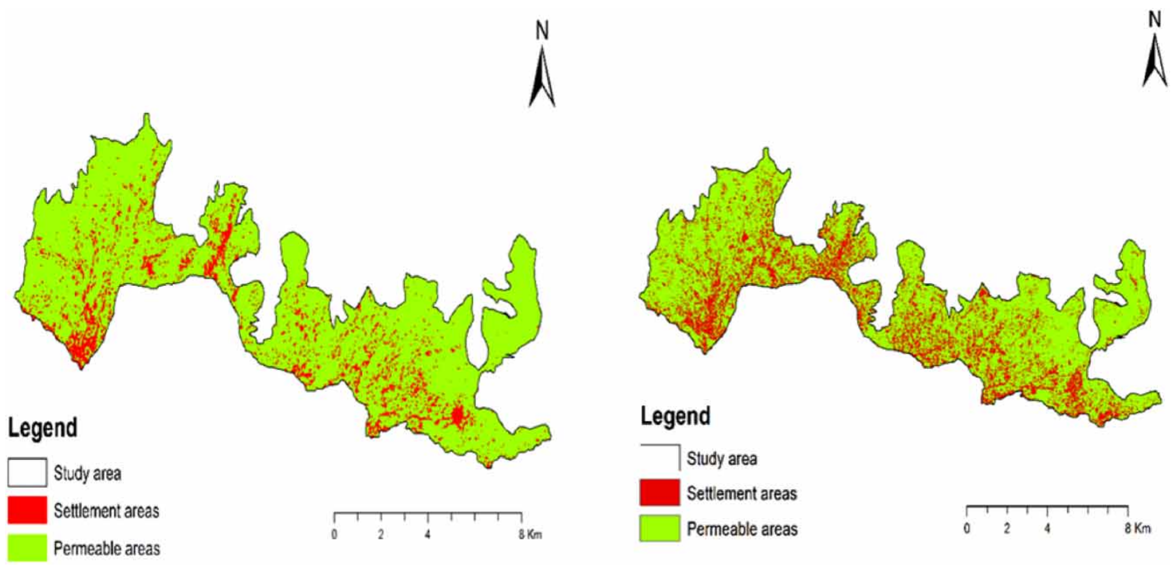

Figure 8 | Land-use change in 2010 and 2020.

Table 4 | Estimated volume of water recharge in 2010, 2020 and 2030

S.No.	Attributes	Years	Slope < 30°
1	Permeable area (km^2)	2010	75.25
		2020	65.61
		2030	57.22
2	Volume of water recharge (MCM/year)	2010	67.73
		2020	59.05
		2030	51.5
3	Deduction (MCM/year)	2010–2020	8.68
		2020–2030	7.55
		2010–2030	16.23

and Pu *et al.* (2020). Increase in urban areas has resulted in a decrease in groundwater volume at a rate of 284.34 MCM, a deficit of 115.34 MCM (a reduction in the groundwater levels of 0.1 m/year) in Oaxaca, Mexico (Olivares *et al.* 2019). Urbanization has led to impervious pavement, causing an effect on surface water systems and groundwater recharge. Decline in rainwater infiltration leads to high runoff, peak discharge flow, then urban flood at downstream areas posing threats to life and property (Pataki *et al.* 2011; Yao *et al.* 2015). Urbanization along with climate change increases these issues even more seriously.

The techniques described by Singh *et al.* (2010), i.e. the 'recharge from field percolation' method, has somewhat similar kinds of recharge processes to those adopted in this research. It is based on deep percolation occurring through cultivated areas from irrigated fields and is the main recharge component, contributing 57% of the total recharge.

The estimated volume of groundwater recharge in this study was greater than that estimated by Lamichhane & Shakya (2020). Since this northern groundwater district is a major aquifer for the KV, estimates may be high. This value is assumed to be the maximum in the permeable areas of KV, whereas other studies (Pandey *et al.* 2013; Shrestha *et al.* 2017) presented the average value for the whole KV. Moreover, the variation in estimates may be due to differences in the approach used and aquifer layers considered (Shrestha *et al.* 2012).

The present study has estimated the potential volume of water recharge based on the permeable area in ideal conditions irrespective of any kind of climatological and hydrological factors. However, earlier studies like Gupta *et al.* (1990); Pandey & Kazama (2011); Shrestha *et al.* (2017); and Lamichhane & Shakya (2020) have mainly focused on rainfall characteristics and different hydrological factors.

The recharge capacity for the study area was estimated to be uniform for all degrees of slopes; however, Adams *et al.* (2004) distinguished the probability of recharge based on it as 100, 95, 75, 50, and 25% for slope degree 0–5, 5–10, 10–20, 20–50, and 50–90, respectively. The double-ring infiltrometer used in the present research mainly favors non-sloppy areas, but it has been used constantly in calculating volume for sloppy areas which might have increased the estimation of the results. Permeable areas with mild slopes hence overestimate the volume of water recharge. This kind of overestimation could be reduced using rain simulators or chemical methods in sloppy areas. In addition, the ring size of the infiltrometer also matters for the accuracy of the infiltration rate. The larger rings would provide high accuracy and smaller ring sizes would give less accuracy. Furthermore, to gain high accuracy in the measurement of recharge volume, seasonal study along with morphological characteristics such as slope, elevation, aspect, curvature, and topographic position index (TPI) that impact infiltration rate will add more knowledge of the hydrology of the northern valley for groundwater recharge and supply.

CONCLUSION

The present study revealed the baseline on the infiltration rate of the northern groundwater district of the KV, which is considered as the groundwater recharge area of the valley, amid the changing land-use pattern. The current study shows a significant impact of land-use on the infiltration rate where higher infiltration rate was observed in the cultivated land compared to the non-cultivated land. Among the different soil properties like pH, moisture, bulk density, organic matter, and soil texture, organic matter was found to impact infiltration rate directly and positively, i.e., land with higher organic matter content has increased infiltration rates and vice versa. In terms of land-use change, 11.78% of permeable land was found to be converted into impervious concrete structures in just a decade (2010–2020), projected to decrease the water volume by 16.23 MCM/year for the period from 2010 to 2030. The double-ring infiltrometer techniques adopted in limited economic conditions in this study were found to be useful in determining the infiltration rate in different land-use types and between various soil components.

The baseline information on the infiltration rate of the study area and estimation of recharge volume with respect to decrease in permeable areas due to urbanization and land-use change are the main outcomes of the present research. The former outcome is important in understanding groundwater reservoirs, designing groundwater management plans, irrigation and drainage systems, and contamination evaluation, whereas the latter is believed to be applied by urban planners to work for the preservation and conservation of permeable areas during urban planning. This field-based assessment coupled with different models of flood helps mitigate and solve urban flooding to some extent, which is emerging in the case of the KV during monsoon. Nevertheless, further field experiments are required to evaluate the impacts of rainfall characteristics in the study area.

ACKNOWLEDGEMENTS

Authors are thankful to the Central Department of Environmental Science, Tribhuvan University, Nepal for providing the platform to carry out the present work. The first author expresses sincere acknowledgement to the National Youth Council, Center of Research for Environment, Energy and Water, and Environment and Public Health Organization for providing an M.Sc. research grant. The authors are grateful to Dr Ramesh Sapkota for his valuable support in the statistical analysis.

DATA AVAILABILITY STATEMENT

All relevant data are included in the paper or its Supplementary Information.

CONFLICT OF INTEREST

The authors declare there is no conflict.

REFERENCES

Abdel-Fattah, M. K., Mohamed, E. S., Wagdi, E. M., Shahin, S. A., Aldosari, A. A., Lasaponara, R. & Alnaimy, M. A. 2021 Quantitative evaluation of soil quality using principal component analysis: the case study of El-Fayoum depression Egypt. *Sustainability* **13**, 1824. https://doi.org/10.3390/su13041824.

Adams, S., Titus, R. & Xu, Y. 2004 *Groundwater Recharge Assessment of the Basement Aquifers of Central Namaqualand. Report to the Water Research Commission*. University of the Western Cape, Bellville.

Alhassoun, R. 2009 *Studies on Factors Affecting the Infiltration Capacity of Agricultural Soils*. Online unter. Available from: https://nbn-resolving.org/urn:nbn:de:gbv:084–27644.

Alley, W. M., Healy, R. W., LaBaugh, J. W. & Relly, T. E. 2002 Flow and storage in groundwater systems. *Science* **296** (5575), 1985–1990. doi:10.1126/science.1067123.

ASTM 2003 *Standard Test Method for Infiltration Rate of Soils in Field Using Double-Ring Infiltrometer*. D-3385-03, ASTM International, 100 Barr Harbor Drive, P.O. Box C700, West Conshohocken, PA 19428-2959, United States. Accessed from: www.astm.rg

Batelaan, O., De Smedt, F. & Trest, L. 2003 Regional groundwater discharge: phreatophyte mapping, groundwater modeling and impact analysis of land use change. *Journal of Hydrology* **275**, 86–108.

Bean, E. Z., Hunt, W. F., Bidelspach, D. A. & Burak, R. J. 2004 Study on the surface infiltration rate of permeable pavements. In: *1st Water and Environment Specialty Conference of the Canadian Society for Civil Engineering (Unpublished)*.

Bobe, B. W. 2004 *Evaluation of Soil Erosion in the Harerge Region of Ethiopia Using Soil Loss Models, Rainfall Simulation and Field Trials*. *Thesis*, Doctor of Philosophy: University of Pretoria, Azania, pp. 83–107.

Bradley, R. M., Weeraratne, S. & Mediwake, T. M. M. 2002 Water use projections in developing countries. *Journal American Water Works Association* **94** (8), 52–63.

Cerda, A. 1996 Seasonal variability of infiltration rates under contrasting slope conditions in southeast Spain. *Geoderma* **69** (3-4), 217–232.

Chancellor, W. J. 1977 *Compaction of Soils by Agricultural Equipment*. Division of Agricultural Sciences, University of California, Bulletin, pp. 50–53.

Chen, Y. J., Day, S. D. & Wick, A. F. 2014 Influence of urban land development and subsequent soil rehabilitation on soil aggregates, carbon, and hydraulic conductivity. *Science of the Total Environment* **494–495**, 329–336. https://doi.org/10.1016/j.scitotenv.2014.06.099.

Cupak, A., Walega, A. & Michalec, B. 2017 Cluster analysis in determination of hydrologically homogeneous regions with low flow. *Acta Scientiarum Polonorum Formatio Circumiectus* **16** (1), 53–63. http://dx.doi.org/10.15576/ASP.FC/2017.16.1.53.

Dahal, A., Khanal, R. & Mishra, B. K. 2019 Identification of critical location for enhancing groundwater recharge in Kathmandu Valley, Nepal. *Groundwater for Sustainable Development* **9**. https://doi.org/10.1016/j.gsd.2019.100253.

Danin, A. & Barbour, M. B. 1982 Microsuccession of cryptogams and phanerogams in the Dead Sea Area, Israel. *Flora* **172** (2), 173–179. https://doi.org/10.1016/S0367-2530%2817%2931325-7.

Diamond, J. & Shanley, T. 2010 Infiltration rate assessment of some soils. *Irish Geography* **36** (1), 32–46. https://doi.org/10.1080/00750770309555810.

Dijkshoorn, J. A. & Huting, J. R. M. 2009 *Soil and Terrain Database for Nepal. Report 2009/01*. ISRIC – World Soil Information, Wageningen, p. 29 with data set. Available from: http:///www.isric.org.

Farid, H. U., Khan, Z. M., Ahmad, I., Shakoor, A., Anjum, M. N., Aqbal, M. M., Mubeen, M. & Asghar, M. 2019 Estimation of infiltration models parameters and their comparison to simulate the onsite soil infiltration characteristics. *International Journal of Agricultural and Biological Engineering* **12** (3), 84–91.

Gautam, D. & Prajapati, R. N. 2014 Drawdown and dynamics of groundwater table in Kathmandu Valley, Nepal. *Open Hydrology Journal* **8**, 17–26.

Gee, G. W. & Bauder, J. W., 1986 Particle size analysis. In: *Methods of Soil Analysis. Physical and Mineralogical Methods* (Klute, A. *et al.*, eds). ASA & SSSA, Madison, WI, pp. 396–400.

Gosling, S. N. & Arnell, N. W. 2016 A global assessment of the impact of climate change on water scarcity. *Climate Change* **134**, 371–385.

Grossman, R. B., Reinsch, T. G., 2002 Bulk density and linear extensibility. In: *Methods of the Soil Analysis Part 4. Physical Methods* (Dane, J. H. & Topp, G. C., eds). Soil Sci. Soc. Am. Book Series No.5, ASA and SSSA, Madison, WI, pp. 201–228.

Gupta, A. G., Poudyal, G. N. & Shrestha, M. N. 1990 Assessing safe yield for groundwater basin in Kathmandu Valley. *AIT Research Report*, November.

Haghnazari, F., Shahgholi, H. & Feizi, M. 2015 Factors affecting the infiltration of agricultural soils: review. *International Journal of Agronomy and Agricultural Research* **6** (5), 21–35.

Harden, C. P. & Scruggs, P. D. 2003 Infiltration on mountain slopes: a comparison of three environments. *Geomorphology* **55**, 5–24.

Horton, R. E. 1933 The role of infiltration in the hydrologic cycle. *Transaction, American Geophysical Union* **14** (1), 446–460.

Hou, X., Zhuang, K. & Liu, A. 2012 Restoration of soil quality after mixed-species planting on mining wasteland at Zijinshan gold-copper mine, Fujian Province, China. *Journal of Agro-Environment Science* **31** (8), 1505–1511.

Igboekwe, M. U. & Adindu, R. U. 2014 Use of Kostiakov's infiltration model on Michael Okpara University of Agriculture, Umudike Soils, Southeastern Nigeria. *Journal of Water Resource and Protection* **6**, 888–894.

Jakeman, A. J., Barreteau, O., Hunt, R. J., Rinaudo, J.-D., Ross, A., Arshad, M., Hamilton, S., 2016 Integrated groundwater management: an overview of concepts and challenges. In: *Integrated Groundwater Management: Concepts Approaches and Challenges* (Jakeman, A. J., Barreteau, O., Hunt, R. J., Rinaudo, J.-D. & Ross, A., eds). Springer International Publishing, Cham, Switzerland, pp. 3–20.

JICA 1990 *Groundwater Management Project in Kathmandu Valley*. Nepal Water Supply Corporation, Kathmandu, Nepal.

Kadam, A. S. 2016 Determination of infiltration rate for site selection of artificial water recharge: an experimental study. *International Journal of Science and Research* **5** (6), 699–705. http://dx.doi.org/10.21275/v5i6.NOV164327.

Kohnke, N. 1968 *Soil Physics*. McGRaw-Hill, New York.

Konikow, L. F. & Kendy, E. 2005 Groundwater depletion: a global problem. *Hydrogeology Journal.* **13**, 317–320.

Kumar, V., Chaplot, B., Omar, P. J., Mishra, S. & Azamathulla, H. M. 2021 Experimental study on infiltration pattern: opportunities for sustainable management in the Northern region of India. *Water Science & Technology* **84**, 10–11.

Kusumandari, A. & Marpaung, P. A. R. 2019 The reduction of infiltration capacity at various tourist attraction areas in Wanagama I Education forest. In *IOP Conf. Series: Earth and Environmental Science*.

KVWSMB 2012 *Groundwater Resources Management Policy*. Kathmandu Valley Water Supply Management Board, Kathmandu, Nepal.

Lamichhane, S. & Shakya, N. M. 2019 Alteration of groundwater recharge areas due to land use/cover change in Kathmandu Valley, Nepal. *Journal of Hydrology: Regional Studies* **26**, 100635. https://doi.org/10.1016/j.ejrh.2019.100635.

Lamichhane, S. & Shakya, N. M. 2020 Shallow aquifer groundwater dynamics due to land use/cover change in highly urbanized basin: the case of Kathmandu Valley. *Journal of Hydrology: Regional Studies* **30**, 100707. https://doi.org/10.1016/j.ejrh.2020.100707.

Linh, P. T., Dung, B. X. & Bao, T. Q. 2018 Infiltration characteristics of soil under Cinnamon and Acacia plantation forest in headwater of Vietnam. *Vietnam Journal of Forest Science* **4**, 83–96.

Loague, K. & Gander, G. A. 1990 Spatial variability of infiltration on a small rangeland catchment. *Water Resources Research* **26**, 957–971.

Mahapatra, S., Jha, M. K., Biswal, S. & Senapati, D. 2020 Assessing variability of infiltration characteristics and reliability of infiltration models in a Tropical Sub-Humid Region of India. *Scientific Reports* **10**, 1515. https://doi.org/10.1038/s41598-020-58333-8.

Masoud, M. H. Z., Basahi, J. M. & Zaidi, F. K. 2019 Assessment of artificial groundwater recharge potential through estimation of permeability values from infiltration and aquifer tests in unconsolidated alluvial formations in coastal areas. *Environmental Monitoring and Assessment*. https://doi.org/10.1007/s10661-018-7173-6.

McDonald, R. I., Douglas, I., Grimm, N. B., Hale, R., Revenga, C., Gronwall, J. & Fekete, B. 2011 Implications of fast urban growth for freshwater provision. *Ambio* **40**, 437–447.

Mireille, N. M., Mwangi, H. M., Mwangi, J. K. & Gathenya, J. M. 2019 Analysis of land use change and its impact on the hydrology of Kakia and Esamburmber Sub-watersheds of Narok County, Kenya. *Hydrology* **6** (4), 86. https://doi.org/10.3390/hydrology6040086.

Mishra, N. & Kumar, S. 2015 Impact of land use change on groundwater recharge in haridwar district. In: *Proceedings of the 20th International Conference on Hydraulics, Water Resources and River Engineering*, 17–19 December, IIT Roorkee, India.

Molina, A., Govers, G., Vanacker, V., Poesen, J., Zeelmaekers, E. & Cisneros, F. 2007 Runoff generation in a degraded Andean ecosystem: interaction of vegetation covers and land use. *Catena* **71**, 357–370.

Moon, S., Woo, N. C. & Lee, K. S. 2004 Statistical analysis of hydrographs and water-table fluctuations to estimate groundwater recharge. *Journal of Hydrology* **292**, 1998–2009.

Nelson, D. W., Sommers, L. E., 1982 Total carbon, organic carbon and organic matter. In: *Methods of Soil Analysis, Part 2* (Page, L., Miller, R. H. & Keeney, D. R., eds). Am. Soc. Agron, Madison, WI, pp. 539–579.

Neris, J., Jimenez, C., Fuentes, J., Morillas, G. & Tejedor, M. 2020 Vegetation and land-use effects on soil properties and water infiltration of Andisols in Tenerife (Canary Islands, Spain). *Catena* **98**, 55–62.

Nileshwari, Y., Pandagale, V. P., Madhuri, G. & Khambalkar, V. P. 2016 Measurement of infiltration on different land covers. *International Journal of Agriculture Sciences* **8**, 2299–2302.

Olivares, E. A. O., Torres, S. S., Jimenez, S. I. B., Enriquez, J. O. C., Zignol, F., Reygadas, Y. & Tiefenbacher, J. P. 2019 Climate change, land use/land cover change, and population growth as drivers of groundwater depletion in the central valleys, Oaxaca, Mexico. *Remote Sensing* **11** (11), 1290. https://doi.org/10.3390/rs11111290.

Orjuela-Matta, H. M., Sanabria, Y. R. & Camacho-Tamayo, J. H. 2012 Spatial analysis of infiltration in an oxisol of the eastern plains of Colombia. *Chilean Journal of Agricultural Research* **72** (3), 404–410.

Osuji, G. E., Okon, M. A., Chukwuma, M. C. & Nwarie, I. I. 2010 Infiltration characteristics of soils under selected land use practices in Owerri, southeastern Nigeria. *World Journal of Agricultural Sciences* **6** (3), 322–326.

Paczynski, B. 1995 *Hydrogeological Atlas of Poland in 1:500000 Scale. Part II. Resources, Quality and Protection of Freshwater*. Polish Geological Institute, Warszawa. (in Polish).

Pandey, V. P. & Kazama, F. 2011 Hydrogeologic characteristics of groundwater aquifers in Kathmandu Valley, Nepal. *Environment Earth Sciences* **62**, 1723–1732.

Pandey, V. P., Chapagain, S. K. & Kazama, F. 2010 Evaluation of groundwater environment of Kathmandu Valley. *Environmental Earth Sciences* **60** (6), 1329–1342.

Pandey, V. P., Shrestha, S. & Kazama, F. 2013 A GIS-based methodology to delineate valley, Nepal. *Applied Water Science* **3**, 453–465.

Pataki, D. E., Carreiro, M. M. & Cherrier, J. 2011 Coupling biogeochemical cycles in urban environments: ecosystem services, green solutions and misconceptions. *Frontiers in Ecology and the Environment* **9** (1), 27–36.

Patle, G. T., Sikar, T. T., Rawat, K. S. & Singh, S. K. 2018 Estimation of infiltration rate from soil properties using regression model for cultivated land. *Geology, Ecology and Landscapes* **3** (2), 1–13. https//doi.org/10.1080.24749508.2018.1481633.

Philip, J. R. 1957 The theory of infiltration: 4. Sorptivity and algebraic infiltration equations. *Soil Science* **84**, 257–264.

Pu, J. H., Pandey, M. & Hanmaiahgari, P. R. 2020 Analytical modeling of sidewall turbulence effect on stream wise velocity profile using 2D approach: a comparison of rectangular and trapezoidal open channel flows. *Journal of Hydro-Environment Research* **32**, 17–25.

Rashidi, M. & Seyfi, K. 2007 Field comparison of different infiltration models to determine infiltration models to determine the soil infiltration for border irrigation method. *American-Eurasian Journal of Agricultural and Environmental Sciences* **2** (6), 628–632.

Scanlon, B. R., Reddy, R. C., Stonestrom, D. A., Prudic, D. E. & Dennehys, K. F. 2005 Impact of land use and land cover change on groundwater recharge and quality in the southwestern US. *Global Change Biology* **11**, 1577–1593.

Setiawan, O., Sartohadi, J., Hadi, M. O. & Mardiatno, D. 2019 Infiltration characterization using principal component analysis and K-means cluster analysis on quaternary volcanic landscape at the southern flank of Rinjani Volcano, Lombok Island, Indonesia. *Physical Geography* **41** (3), 217–237. https://doi.org/10.1080/02723646.2019.1620526.

Shakya, B. M., Nakamura, T. & Shrestha, S. D. 2019 Identifying the deep groundwater recharge processes in an intermountain basin using the hydrogeochemical and water isotope characteristics. *Hydrology Research* **50** (5), 1216–1229.

Shrestha, R. R. 2009 *Water Storage 'Rainwater Harvesting and Groundwater Recharge for Water Storage in the Kathmandu Valley'*. ICIMOD.

Shrestha, S. & Kafle, G. 2020 Variation of selected physicochemical and hydrological properties of soils in different tropical land use systems of Nepal. *Applied and Environmental Soil Science*. Article ID 8877643. https://doi.org/10.1155/2020/8877643.

Shrestha, S. R. & Shah, S. 2014 *Shallow Aquifer Mapping of Kathmandu Valley*. Ground Resources Development Board, Babarmahal, Kathmandu. (Unpublished).

Shrestha, S., Pradhananga, D. & Pandey, V. P. 2012 *Kathmandu Valley Groundwater Outlook*. Asian Institute of Technology (AIT), The Small Earth Nepal (SEN), Center of Research for Environment Energy and Water (CREEW), International Research Center for River Basin Environment-University of Yamanashi (ICRE-UY), Kathmandu, Nepal.

Shrestha, S., Kafle, R. & Pandey, V. P. 2017 Evaluation of index-overlay methods for groundwater vulnerability and risk assessment in Kathmandu Valley, Nepal. *Science of the Total Environment* **575**, 779–790. https://doi.org/10.1016/j.scitotenv.2016.09.141.

Singh, A., Krause, P., Panda, S. & Flugel, W. A. 2010 Rising water table: a threat to sustainable agriculture in an irrigated semi-arid region of Haryana, India. *Agricultural Water Management* **97**, 1443–1451.

Sonaje, S. P. 2013 Modeling of infiltration process: a review. *Indian Journal of Applied Research* **3** (9), 226–230.

Stasko, S., Tarka, R. & Olichwer, T. 2012 *Groundwater Recharge Evaluation Based on the Infiltration Method*. Institute of Geological Sciences, Wroclaw University, Poland. Maloszewski.

Tiwari, K., Sitaula, B. K., Borresen, T. & Bajracharya, R. M. 2006 An assessment of soil quality in Powalker khare khola watershed of the middle mountains in Nepal. *Journal of Food, Agriculture & Environment* **4**, 276–283.

Turner, E. R. 2006 *Comparison of Infiltration Equations and their Field Validation with Rainfall Simulation*. Thesis (MSc.), University of Maryland, USA.

Tyagi, N. K., Sharma, D. K. & Luthra, S. K. 2000a Determination of evapotranspiration and crop coefficients of rice and sunflower. *Agricultural Water Management* **45**, 41–54.

Tyagi, N. K., Sharma, D. K. & Luthra, S. K. 2000b Evapotranspiration and crop coefficient of wheat and sorghum. *Journal of Irrigation and Drainage Engineering* **126** (4), 215–222.

Verbist, K., Torfs, S., Cornelis, W. M., Oyarzun, R., Sato, G. & Gabriels, D. 2010 Comparison of single- and double- ring infiltrometer methods on stony soils. *Vadose Zone Journal* **9** (2), 462–447. https://doi.org/10.2136/vzj2009.0058.

Walker, W. R., Prestwich, C. & Spofford, T. 2006 Development of the revised USDA-NRCS intake families for surface irrigation. *Agricultural Water Management* **85** (1-2), 157–164.

Wang, W. & Zhang, J. 1991 Research on field soil water penetration testing devices. *Acta Conservations Solt et Aquae Sinica* **5** (4), 38–44.

Wang, B., Jin, M., Nimmo, J. R., Yang, L. & Wang, W. 2008 Estimating groundwater recharge in Hebei Plain, China under varying land use practices using tritium and bromide tracers. *Journal of Hydrology* **356**, 209–222.

Wang, P., Zheng, H., Ren, Z., Zhang, D., Zhai, C., Mao, Z., Tang, Z. & He, X. 2018 Effects of urbanization, soil property and vegetation configuration on soil infiltration of urban forest in Changchun, Northeast China. *Chinese Geographical ScienceI* **28**, 482–494. http://dx.doi.org/10.1007/s11769-018-0953-7.

Waxman, S. & Stevens, K. R. 1930 A critical study of the methods of determining the nature and abundance of soil organic matter. *Soil Science* **30**, 97–116.

Weber, H. & Sciubba, J. D. 2018 The effect of population growth on the environment: evidence from European regions. *European Journal of Population* **35**, 379–402.

Yao, L., Chen, L. D. & Wei, W. 2015 Potential reduction in urban runoff by green spaces in Beijing: a scenario analysis. *Urban Forestry & Urban Greening* **142** (2), 300–308.

Yasin, H. I. & Ghazal, E. M. 2021 Infiltration and some physical properties of soil. *Al-Rafidain Engineering Journal* **26** (2), 249–258.

Yimer, F., Messing, I., Ledin, S. & Abdelkadir, A. 2008 Effects of different land use types on infiltration capacity in a catchment in the highlands of Ethiopia. *Soil Use and Management* **24**, 344–349.

Zhou, F., Xu, Y., Chen, Y., Xu, C.-Y., Gao, Y. & Du, J. 2013 Hydrological response to urbanization at different spatio-temporal scales simulated by coupling of CLUE-S and the SWAT model in the Yangtze River Delta region. *Journal of Hydrology* **485**, 113–125.

First received 31 August 2022; accepted in revised form 30 December 2022. Available online 12 January 2023